Centrality and Transverse Momentum Dependence of Collective Flow in 158 A GeV Pb+Pb Collisions Measured via Inclusive Photons

WA98 Collaboration

M.M. Aggarwal [a] , Z. Ahammed [k] , A.L.S. Angelis [b] * , V. Antonenko [c] , V. Arefiev [d] , V. Astakhov [d] , V. Avdeitchikov [d] , T.C. Awes [e] , P.V.K.S. Baba [f] , S.K. Badyal [f] , S. Bathe [g] , B. Batiounia [d] , T. Bernier [h] , V.S. Bhatia [a] , C. Blume [g] , D. Bucher [g] , H. Büsching [g] , L. Carlén [j] , S. Chattopadhyay [k] , M.P. Decowski [ℓ] , H. Delagrange [h] , P. Donni [b] , M.R. Dutta Majumdar [k] , A.K. Dubey [s] , K. El Chenawi [j] , K. Enosawa [m] , S. Fokin [c] , V. Frolov [d] , M.S. Ganti [k] , S. Garpman [j] * , O. Gavrishchuk [d] , F.J.M. Geurts [n] , T.K. Ghosh [o] , R. Glasow [g] , B. Guskov [d] , H. Å.Gustafsson [j] , H. H.Gutbrod [p] , I. Hrivnacova [q] , M. Ippolitov [c] , H. Kalechofsky [b] , R. Kamermans [n] , K. Karadjev [c] , K. Karpio [r] , B. W. Kolb [p] , I. Kosarev [d] , I. Koutcheryaev [c] , A. Kugler [q] , P. Kulinich [ℓ] , M. Kurata [m] , A. Lebedev [c] , H. Löhner [o] , L. Luquin [h] , D.P. Mahapatra [s] V. Manko [c] , M. Martin [b] , G. Martínez [h] , A. Maximov [d] , Y. Miake [m] , G.C. Mishra [s] , B. Mohanty [s] , M.-J. Mora [h] , D. Morrison [t] , T. Mukhanova [c] , D. S. Mukhopadhyay [k] , H. Naef [b] , B. K. Nandi [s] , S. K. Nayak [f] , T. K. Nayak [k] , A. Nianine [c] , V. Nikitine [d] , S. Nikolaev [c] , P. Nilsson [j] , S. Nishimura [m] , P. Nomokonov [d] , J. Nystrand [j] , A. Oskarsson [j] , I. Otterlund [j] , T. Peitzmann [n] , D. Peressounko [c] , V. Petracek [q] , S.C. Phatak [s] , W. Pinganaud [h] , F. Plasil [e] , M.L. Purschke [p] , J. Rak [q] , R. Raniwala [i] , S. Raniwala [i] , N.K. Rao [f] , F. Retiere [h] , K. Reygers [g] , G. Roland [ℓ] , L. Rosselet [b] , I. Roufanov [d] , C. Roy [h] , J.M. Rubio [b] , S.S. Sambyal [f] , R. Santo [g] , S. Sato [m] , H. Schlagheck [g] , H.-R. Schmidt [p] , Y. Schutz [h] , G. Shabratova [d]

, T.H. Shah [f] , I. Sibiriak [c] , T. Siemiarczuk [r] , D. Silvermyr [j] ,
B.C. Sinha [k] , N. Slavine [d] , K. Söderström [j] , G. Sood [a] ,
S.P. Sørensen [t] , P. Stankus [e] , G. Stefanek [r] , P. Steinberg [ℓ] ,
E. Stenlund [j] , M. Sumbera [q] , T. Svensson [j] , A. Tsvetkov [c] ,
L. Tykarski [r] , E.C.v.d. Pijll [n] , N.v. Eijndhoven [n] ,
G.J.v. Nieuwenhuizen [ℓ] , A. Vinogradov [c] , Y.P. Viyogi [k] ,

A. Vodopianov [d] , S. Vörös [b] , B. Wysłouch [ℓ] , G.R. Young [e]

[a] *University of Panjab, Chandigarh 160014, India*

[b] *University of Geneva, CH-1211 Geneva 4,Switzerland*

[c] *RRC "Kurchatov Institute", RU-123182 Moscow, Russia*

[d] *Joint Institute for Nuclear Research, RU-141980 Dubna, Russia*

[e] *Oak Ridge National Laboratory, Oak Ridge, Tennessee 37831-6372, USA*

[f] *University of Jammu, Jammu 180001, India*

[g] *University of Münster, D-48149 Münster, Germany*

[h] *SUBATECH, Ecole des Mines, Nantes, France*

[i] *University of Rajasthan, Jaipur 3020inst4, Rajasthan, India*

[j] *Lund University, SE-221 00 Lund, Sweden*

[k] *Variable Energy Cyclotron Centre, Calcutta 700 064, India*

[ℓ] *MIT Cambridge, MA 02139, USA*

[m] *University of Tsukuba, Ibaraki 305, Japan*

[n] *Universiteit Utrecht/NIKHEF, NL-3508 TA Utrecht, The Netherlands*

[o] *KVI, University of Groningen, NL-9747 AA Groningen, The Netherlands*

[p] *Gesellschaft für Schwerionenforschung (GSI), D-64220 Darmstadt, Germany*

[q] *Nuclear Physics Institute, CZ-250 68 Rez, Czech Rep.*

[r] *Institute for Nuclear Studies, 00-681 Warsaw, Poland*

[s] *Institute of Physics, 751-005 Bhubaneswar, India*

[t] *University of Tennessee, Knoxville, Tennessee 37966, USA*

* *Deceased*

Abstract

Directed and elliptic flow of inclusive photons near mid-rapidity in 158A GeV Pb+Pb collisions has been studied. The data have been obtained with the photon spectrometer LEDA of the WA98 experiment at the CERN SPS. The flow strength has been measured for various centralities as a function of p_T and rapidity over $0.18 < p_T < 1.5\,\mathrm{GeV}/c$ and $2.3 < y < 2.9$. The angular anisotropy has been studied relative to an event plane obtained in the target fragmentation region that shows the elliptic flow to be in-plane. The elliptic flow has also been studied using two-particle correlations and shown to give similar results. A small directed flow component is observed. Both the directed and elliptic flow strengths increase with p_T. The photon flow results are used to estimate the corresponding neutral pion flow.

Key words: ultrarelativistic heavy-ion collisions, collective flow, inclusive photons

1 Introduction

Heavy ion collisions at relativistic energies provide a means to study the properties of nuclear matter at high temperature and density. In such collisions it is expected that a high density interaction zone is formed. If this system thermalizes, the thermal pressure will generate collective transverse expansion [1]. Such collective flow, and especially its anisotropy, will reflect the time evolution of the pressure gradients of the system and can provide information on the equation of state (EOS) in the initial phase [2,3] and during the expansion [4], and in particular about the possible formation of the Quark Gluon Plasma (QGP) [5,6].

QGP formation requires high energy density and local thermalisation of the system. While transverse energy measurements indicate the attainment of high energy densities [7], the degree of thermalization has not been unambiguously determined. Measurements of collective flow may be one of the strongest hints related to the degree of thermalisation. One may consider two extreme cases: the low density limit, where the mean free path is comparable or larger than the system size for which cascade models may be appropriate, and the hydrodynamic limit, where the mean free path of the particles is much less than the system size. The study of collective flow as a function of beam energy and system size, transverse and longitudinal momentum, and particle species may allow to separate these two scenarios and to recognize the hadronic or partonic (QGP) nature of the reaction [8].

The anisotropic flow of charged fragments has been measured in nuclear collisions at various beam energies: at 0.1–1.0 A GeV [9,10,11], at 10A GeV [12], at 158A GeV [13,14,15,16,17] and also at $\sqrt{s_{NN}} = 130$ and 200 GeV [18,19,20]. The first p_T-integrated photon flow measurement was performed by the WA93 experiment [15] for 200 A GeV S+Au collisions, where photons were measured with the Photon Multiplicity Detector (PMD). In the present work we report first results of photon collective flow measurements in 158 A GeV Pb+Pb collisions using photons identified and momentum analyzed in the lead glass calorimeter LEDA of the WA98 experiment. Preliminary results have been presented in [21,22].

2 Experimental Setup

The data presented here were obtained in the WA98 experiment [23] for 158 A GeV Pb+Pb collisions at the CERN SPS. The WA98 setup consisted of large acceptance hadron and photon spectrometers, calorimeters for forward and transverse energy measurements, and detectors for photon and charged

particle multiplicity measurements.

The centrality of the event was determined by the total transverse energy, E_T, measured with the mid-rapidity calorimeter (MIRAC) [24], which covered the pseudo-rapidity range of $3.5 < \eta < 5.5$. It was placed at 24.7 meters downstream from the target and consisted of 30 stacks, each divided vertically into 6 towers, of size 20 x 20 cm^2 each. The MIRAC measured both the transverse electromagnetic E_T^{em} and hadronic E_T^{had} energies. Events with large E_T correspond to the most central collisions with small impact parameter. The minimum bias trigger required a beam trigger with a MIRAC transverse energy greater than a low threshold.

The Plastic Ball spectrometer, used for the reaction plane (RP) determination, had full azimuthal coverage in the pseudorapidity range of $-1.7 < \eta < 0.5$ (i.e. in the target fragmentation region with polar angles $70^\circ < \theta < 160^\circ$). It consisted of 655 detector modules and allowed to identify pions, protons, deutrons, tritons, ^{3}He, and ^{4}He with kinetic energies of 50 to 250 MeV by the $\Delta E - E$ method. Each module comprised a slow 4 mm thick CaF_2 ΔE scintillator followed by a fast plastic scintillator, both read out by a common photomultiplier [25].

Photons, of which $\sim 85\%$ originate from π^0 decay [26], were detected in the electromagnetic calorimeter LEDA, a highly segmented photon detector located 22.1 m downstream of the target and covering the photon rapidity region $2.3 < y < 2.9$, i.e. backwards of mid-rapidity ($y = 2.9$). LEDA consisted of 10080 TF1 lead-glass modules, read out by FEU-84 photomultipliers. The photomultiplier high voltage was generated on-base with custom developed [27] Cockcroft-Walton voltage-multiplier type bases which were individually controlled by a VME processor. The photomultiplier signals were digitized with a custom-built ADC system [28]. The dimensions of each module were 4x4x40 cm^3 (14.3 radiation lengths depth and 1.1 Moliere radius width). Each group of 24 modules had its own calibration and gain monitoring system based on a set of 3 LEDs mounted inside a sealed reflecting cover dome. Each module viewed the reflected LED light through an aperture on the front surface, while the LED light was simultaneously monitored by a PIN-photodiode [29].

LEDA was calibrated with 10 GeV electrons in the X1 beam at the CERN SPS in the years 1993-1994. Electron beams with energies from 3 GeV to 20 GeV were used to measure the energy and position resolution, and the energy non-linearity. The measured energy resolution was $\sigma/E = (5.5\pm0.6)\%/\sqrt{E}+(0.8\pm 0.2)\%$ and the measured position resolution was $\sigma/E = (8.35\pm0.25)\text{mm}/\sqrt{E}+ (0.15 \pm 0.07)\text{mm}$. A more detailed description of the WA98 setup is given in [16,23,26].

3 The Methods

Two complementary methods have been used in this analysis of anisotropic flow: the study of single-particle angular distributions with respect to an estimated reaction plane (*reaction plane method*) and the study of two-particle correlations (*correlation method*). Both methods assume that the underlying azimuthal distribution of particles with respect to the reaction plane (RP), which is the plane that contains the impact parameter and beam direction vectors, can be described by a Fourier decomposition:

$$\frac{1}{N}\frac{dN}{d(\phi - \Psi_{RP})} = 1 + 2v_1 \cos\left(\phi - \Psi_{RP}\right) + 2v_2 \cos\left(2(\phi - \Psi_{RP})\right), \qquad (1)$$

where ϕ is the azimuthal angle of the emitted particle, and Ψ_{RP} is the azimuthal angle of the RP. The anisotropic flow is characterized by the values of the Fourier coefficients v_1, for directed flow, and v_2, for elliptic flow.

3.1 The Reaction Plane Method

The conventional reaction plane method [30,31] uses the distribution of particles in their azimuthal angle relative to the estimated reaction plane. Because the true reaction plane is not known in the experiment, one has to establish an *event plane* (EP) from the measured particles as an estimate for the reaction plane.

Particles measured in the target fragmentation region show significant directed flow – proton, deuterons, and heavier fragments are emitted in the reaction plane in one direction, while pions are emitted in the opposite direction, as has been measured with the Plastic Ball detector [32]. This information has been used to calculate an event plane angle from the particles measured in the Plastic Ball:

$$\Phi_{EP} = \tan^{-1}\left(\frac{\sum_{i=1}^{N} E_T^i \sin\phi_i}{\sum_{i=1}^{N} E_T^i \cos\phi_i}\right), \qquad (2)$$

where the sum runs over all fragments and identified positive pions. E_T^i and ϕ_i are the transverse kinetic energy and azimuthal angle in the laboratory frame of the $i-$th particle, respectively. For pions, ϕ was replaced by $\phi + \pi$ to account for the opposite sign pion directed flow [32].

The azimuthal distribution of photons detected by the LEDA calorimeter has been studied relative to this event plane angle. The distributions are studied

as a function of $\Delta\Phi = \phi_\gamma - \Phi_{EP}$ and are fitted with:

$$\frac{1}{N}\frac{dN}{d\Delta\Phi} = 1 + 2v_1^{obs}\cos(\Delta\Phi) + 2v_2^{obs}\cos(2\Delta\Phi)\,. \tag{3}$$

The measured EP doesn't coincide exactly with the true RP because of the finite number of detected particles and resulting fluctuations. Because of this finite reaction plane resolution, the coefficients obtained from the fits have to be corrected by dividing them by the event plane resolution correction factors (RCF_n):

$$v_n = \frac{v_n^{obs}}{RCF_n}. \tag{4}$$

The resolution correction functions RCF_n are given by [31]:

$$\begin{aligned} RCF_n &= \langle\cos(n(\Phi_{EP} - \Psi_{RP}))\rangle \\ &= \frac{\sqrt{\pi}}{2\sqrt{2}}\chi_m \exp\left(\frac{-\chi_m^2}{4}\right)\left[I_{\frac{k-1}{2}}\left(\frac{\chi_m^2}{4}\right) + I_{\frac{k+1}{2}}\left(\frac{\chi_m^2}{4}\right)\right] \end{aligned} \tag{5}$$

where Ψ_{RP} is the true RP angle, χ_m is the resolution parameter, which is proportional to the square root of the multiplicity, m is the order of the Fourier component used for calculation of the event plane and $k = n/m$.

Since Ψ_{RP} is unknown, the RCF's must be determined from the measured EP themselves. This can be done by a subevent analysis in which each event, in this case consisting of hits in the Plastic Ball detector, is randomly divided into two subevents (A and B) and for each subevent the EP angle Φ_{EP} (Φ_A or Φ_B) is calculated. The quantity $\langle\cos(n(\Phi_A - \Phi_B))\rangle$ is determined directly from the subevent correlation function. It is then used in equation 5 to obtain the parameter χ_m^{sub} for the subevent multiplicity, which is then used to calculate $\chi_m = \sqrt{2}\chi_m^{sub}$ for the full event, and finally to obtain RCF_n. In this analysis we have used $m = 1$ ($k = 1$) for RCF_1 and for RCF_2 ($k = 2$).

3.2 The Correlation Method

Alternatively, the flow values have been obtained from the azimuthal correlations of photon pairs as described in [2,31,33,34,35]. The correlation function is calculated as:

$$C_{\gamma\gamma}(\Delta\phi) \equiv \frac{d^2N/d\phi_1 d\phi_2}{dN/d\phi_1 \cdot dN/d\phi_2}, \tag{6}$$

where $\Delta\phi = \phi_1 - \phi_2$. The $C_{\gamma\gamma}$ are calculated as the ratio of the true two-photon distribution to the pair distribution from mixed events. This is necessary to correct for distortions from the limited acceptance of the photon detector. In the event-mixing procedure we have taken care to mix only events with similar global properties and to use identical cuts, especially regarding the two-cluster separation within the detector. The two-photon correlation functions have then been fitted with:

$$C_{\gamma\gamma}(\Delta\phi) = 1 + 2v_1^2 \cos(\Delta\phi) + 2v_2^2 \cos(2(\Delta\phi)). \quad (7)$$

From these fits, no significant v_1 component was observed. Since very little directed flow is expected near mid-rapidity, we have set $v_1 \equiv 0$ in this analysis.

If collective flow is dominant, this method should be equivalent to the previous one since (a) the correlation between every particle and the RP induces a correlation amongst the particles, and (b) correlating two subevents amounts to summing two-particle correlations [36]. The correlation method has the advantage that no EP determination, and therefore no resolution correction, is needed. However, non-flow correlations, such as back-to-back correlations due to momentum conservation [22], should be taken into account.

4 Analysis

The data presented here were taken in 1995 and 1996 with the 158 A GeV Pb ion beams of the CERN SPS. Pb targets of 495 and 239 mg/cm^2 thickness were used. About 10^7 events were analyzed. The events were divided into 8 centrality classes defined by intervals in the total E_T measured by MIRAC, as summarized in Table 1. The centralities are expressed as fractions of the minimum bias cross sections as a function of the total E_T, measured by MIRAC. In addition, a multiplicity of greater than 3 fragments measured in the Plastic Ball was demanded to allow for a reasonable determination of the EP. This has a significant effect for the peripheral bins and causes a slight bias towards higher multiplicity within the bin.

In addition to the 8 classes of centrality shown in Table 1, studies were performed with combined centrality classes: 2 + 3 (47–83%), 4 + 5 + 6 (13–47%) and 7 + 8 (0–13%). The table also shows the number of participants N_{part} as calculated in a Glauber type calculation discussed in [37].

To further suppress the hadron contamination in the photon sample, only those showers in the calorimeter have been used which satisfy the following cuts:

E_T class		E_T (GeV)	N_{part}
1	$83-100\%$	$0-28.35$	10 ± 2
2	$65-83\%$	$28.35-79.05$	28 ± 2
3	$47-65\%$	$79.05-161.55$	63 ± 2
4	$24-47\%$	$161.55-281.05$	133 ± 3
5	$19-24\%$	$281.05-318.05$	205 ± 2
6	$13-19\%$	$318.05-361.55$	247 ± 2
7	$6.5-13\%$	$361.55-410.95$	291 ± 2
8	$0-6.5\%$	> 410.95	351 ± 1

Table 1
Centrality classes used in this analysis. The percentage of the measured minimum bias cross section included in each class is given. Also given is the corresponding average number of participants for each class with an estimate of the systematic error. Cuts on E_T are for 1995 data set, 1996 data set cuts are shown in [38].

- The measured energy was greater than 0.75 GeV. This cut suppressed minimum ionizing particles.
- The lateral dispersion of the shower was less than a maximum value. This suppressed showering hadrons.

These cuts kept the hadron contamination in the photon sample to less than $\approx 7\%$ [26,39].

The observed raw Φ_{EP}-distributions showed a variation due to detector biases, such as dead channels and inefficiency, of less than 5%. This non-uniformity has to be removed before extracting the flow strength from the measured correlation functions. This has been done by two methods:

- The real distribution was divided by the equivalent distribution for mixed events, where ϕ_γ and Φ_{EP} are taken from different events.
- In accumulating the distributions, the entries were weighted with the inverse of the Φ_{EP} distribution.

Both methods gave consistent results within errors, we have used the second method for the final result.

Fig. 1 (left) shows examples of the measured photon azimuthal correlation functions for different centralities. A clear modulation is seen, especially in the semi-central classes, which can be described well with fits to equation 3.

The resolution correction factors RCF's for each centrality were determined as described above from the subevent correlation functions as shown in Fig. 1

(right). In this case the Plastic Ball acceptance correction was done by using mixed subevents, i.e. subevents from different events. The deviation of the mixed subevents from unity, i.e. the order of magnitude of this correction, was less than 2% (as shown in Fig. 1 (right)).

Fig. 2a shows the values of the resolution correction factors RCF's determined in this way as a function of the number of participants. A stronger subevent correlation implies a better determination of the RP, and the corresponding values of the RCF's are larger [40]. It is seen, that the subevent correlation is strongest for semi-central events, whereas for peripheral and central events the quality of the EP - determination is worse. The RCF's shown in Fig. 2a have been obtained for the 1996 beam time. The RCF's have been calculated and applied independently for the 1995 beam time, with values found to be smaller by $\sim 20 - 40\%$.

The v_2 elliptic flow values for photons have also been obtained from the two-photon correlation functions for various centrality classes, although not all of these precisely match those used for the reaction plane method analysis [41]. The v_2 elliptic flow values for photons obtained by the two methods are compared in Figs. 2b and 3. The two photon correlation functions have been fitted with Eq. 7 to extract v_2 with $v_1 \equiv 0$. Fig. 2b shows the centrality dependence of v_2 integrated over $p_T > 0.18$ GeV/c. The solid circles are the values obtained from the reaction plane method and the open circles are those from the correlation method. For centralities corresponding to $N_{part} > 50$ there is very good agreement between the two methods. Fig. 3 shows the elliptic flow as a function of p_T for central and two semi-central classes. There is good agreement between the methods.

One should note that the most peripheral classes suffer from several problems: The determination of the reaction plane has a large uncertainty, especially fluctuations due to the low multiplicity play a role here. In addition, for the correlation method it has been seen that there may be considerable non-flow components for these centralities [22] which would influence the extraction of the flow. Furthermore, we have neglected directed flow in the correlation method which may also lead to systematic errors in the v_2 determination. The results from the reaction plane method are used in the discussions that follow.

As a consistency check we have performed the reaction plane analysis independently on the data from the two different beam periods, where the quality of the RP determination was found to be different. The resulting flow values are in good agreement.

5 Systematic Error

The systematic errors of the obtained coefficients include:

- uncertainties in the event plane determination in the Plastic Ball due to non-uniformity of acceptance and efficiency or imperfect particle identification, estimated as $< 2\%$.
- uncertainties in the photon angular distributions due to charge particle contamination of photons in LEDA. This contamination is less than $\approx 7\%$ ([26]). The uncertainties are related to a difference in the observed flow between charged pions and pion decay photons and were estimated as $< 3.5\%$.

Other sources of the systematic errors have been investigated by comparing the results obtained under different conditions. The following checks have been performed:

(1) Different weights (E_T vs. p_T) have been used for the determination of the event plane.
(2) Different acceptance regions of the Plastic Ball detector ($70^\circ < \theta < 160^\circ$ or $60^\circ < \theta < 160^\circ$) have been used.
(3) Different identification cuts for the Plastic Ball fragments were used.
(4) The event plane was determined with and without including pions in the Plastic Ball.
(5) Results of the two different beam periods were analyzed separately.

Another possible contribution to the systematic error is due to non-flow correlations. Among such non-flow effects relevant for azimuthal correlations are the correlations due to momentum conservation, long- and short-range two- and many-particle correlations (due to quantum statistics, resonances, jet or mini-jet production, etc.). The contribution of non-flow correlations scales as $1/N$, where N is the multiplicity of particles used to determine the event plane. The "momentum conservation" contribution increases with the fraction of particles detected, and the relative contribution of Bose-Einstein correlations would be independent of N. The effect of non-flow correlations in the reaction plane method is expected to be small as the event plane is determined from particle which have a large pseudorapidity separation $\Delta\eta > 1.8$ from the photons. The non-flow contributions to the event plane determination have been investigated by studying the dependence of the RCF's on the Plastic Ball multiplicity. The conventional subevent analysis was performed excluding various fractions of the Plastic Ball particles to investigate the deviation of the flow parameter χ_m from $\chi_m \approx \sqrt{N}$ (see eq. 5).

All of these systematic checks lead to a total systematic error estimate of less than $\pm 17\%$ for both measured values of the flow coefficients. Unless explicitly stated otherwise, the systematic errors are not included in the figures.

6 Results

Fig. 4a,b shows the final values of the directed flow v_1 and the elliptic flow v_2 coefficients as a function of the number of participants. The data were integrated over $p_T > 0.18\,\mathrm{GeV}/c$ and over rapidity $y = 2.3 - 2.9$.

Both types of flow decrease in strength with the number of participants. The sign of all values is positive with the sign convention that positive v_1 corresponds to the directed flow direction of the protons in the projectile fragmentation direction and positive v_2 corresponds to the in-plane direction. Thus, the directed flow of photons below mid-rapidity is in the same direction as the directed flow of pions, oppositee to the protons, in the target fragmentation region, and the elliptic flow is oriented in the reaction plane.

The transverse momentum dependence of the photon flow integrated over $y = 2.3 - 2.9$ is shown in Fig. 4c,d for different centrality classes. Both flow coefficients show an increase with p_T which is compatible with a blast wave behavior (see below,[19], [42]).

To be able to compare the flow of photons to other experimental results we have attempted to establish the relation between the observed photon flow and the underlying flow of the parent neutral pions. This has been investigated in Monte-Carlo simulations. In the simulations, π^0's were generated according to the p_T spectrum measured by WA98 [26]. The π^0 azimuthal distributions were modulated with directed and elliptic flow components. The values of the π^0 v_1 and v_2 and their p_T-dependence have been constrained by the photon measurement. The p_T-dependence of the azimuthal asymmetry has been parameterized following a simple hydrodynamically motivated blast wave model, described in [19],[43], and generalized in [42] to also describe v_1 :

$$v_n(p_T) = \frac{\int_0^{2\pi} d\phi_b \cos(n\phi_b) I_n(\alpha) K_1(\beta)[1 + 2s_n \cos(n\phi_b)]}{\int_0^{2\pi} d\phi_b I_0(\alpha) K_1(\beta)[1 + 2s_n \cos(n\phi_b)]} \tag{8}$$

where the harmonic n can be either 1 or 2, I_0, I_n, and K_1 are the modified Bessel functions, $\phi_b = \phi - \Psi_{RP}$, $\alpha(\phi_b) = (p_T/T_f)\sinh[\rho(\phi_b)]$, $\beta(\phi_b) = (m_T/T_f)\cosh[\rho(\phi_b)]$, s_n is the surface emission parameter, and T_f is the freeze-out temperature. The azimuthal flow rapidity is given as $\rho(\phi_b) = \rho_0 + \rho_a \cos(n\phi_b)$ with ρ_0 is the mean transverse expansion rapidity ($v_0 = \tanh[\rho_0]$) and ρ_a is the amplitude of its azimuthal variation, respectively. Further details are given in [42].

Without regard to the physical interpretation of the parameters of this model

it can be used to provide a convenient parameterization of the p_T dependence of the flow. For this purpose Eq. 8 can be further simplified by setting $\rho_a = 0$. The integrals can be solved to reduce the expression to two parameters, a_n and b_n. The expressions for the p_T dependence of the directed and elliptic flow are then:

$$v_1(p_T) = a_1 \frac{I_1(b_1 p_T)}{I_0(b_1 p_T)} \tag{9}$$

$$v_2(p_T) = a_2(1 - 2\frac{I_1(b_2 p_T)}{b_2 p_T I_0(b_2 p_T)}) \tag{10}$$

The measured photon $v_n(p_T)$ are described well by these expressions (see Fig. 4c,d). The extracted a_n and b_n were constrained to have a smooth centrality dependence.

The simulated π^0 p_T distributions have been parameterized as:

$$\frac{1}{N_{Event}} \frac{d^2N}{dydp_T} = \frac{1}{N_{Event}} E \frac{d^3N}{dp^3} p_T = C' p_T \left(\frac{p'_0}{p'_0 + p_T} \right)^{n'} \tag{11}$$

with parameters C', p'_0, n' taken from the measured π^0 results ([26]). Jetset 7.4 was used to generate the π^0-decay photons which were then filtered in the simulations with the detector acceptance and efficiency.

In the simulations, the π^0's were generated with an azimuthal asymmetry with p_T dependent v_n parameterized by Eqs. 9 and 10. As an initial ansatz, the measured photon $v_n = g(p_T)$ for each centrality was used for the $v_n = f(p_T)$ of the simulated pions. The output $v_n = g'(p_T)$ of the simulated decay photons was compared to the measured photon dependence and used to adjust the π^0 v_n for the next iteration. The procedure was iterated until the simulated and measured photon results were in agreement, which typically required two to three iterations. The a_n and b_n coefficients obtained from the fit to the photon results and the coefficients extracted for the π^0's by the iteration procedure are summarized in Table 2. The ratio of the flow coefficients extracted for the simulated decay photons to the input pion flow coefficients provided the correction factors $k_n(p_T) = v_n^\gamma(p_T)/v_n^\pi(p_T)$ used to extract the π^0 v_n from the measured photon v_n for $p_T > 0$ GeV/c. The systematic errors on the k_n were determined from the uncertainties Δ of the fit parameters: $a_n \pm \Delta a_n$, $b_n \pm \Delta b_n$, $p'_0 \pm \Delta p'_0$ and $n' \pm \Delta n'$. Within errors, the final results were found to be consistent with an analysis in which a simple linear p_T dependence of the $v_n^\pi(p_T)$ was assumed.

	Fit to γ				Extracted for π^0			
Centrality	a_1	b_1	a_2	b_2	a_1	b_1	a_2	b_2
1	0.008	3.06	0.255	5.3	0.005	3.19	0.335	3.046
2	0.0075	3.06	0.24	5.25	0.0075	3.06	0.29	3.217
3	0.0072	3.06	0.22	5.2	0.0072	3.06	0.28	3.09
4	0.006	3.06	0.17	5.1	0.0078	3.06	0.217	2.98
5	0.005	3.06	0.12	5.0	0.005	3.256	0.158	2.87
6	0.0045	3.06	0.095	4.9	0.0044	3.06	0.118	2.93
7	0.004	3.06	0.06	4.8	0.0042	3.06	0.068	3.1
8	0.003	3.06	0.03	4.7	0.0026	3.06	0.028	3.8

Table 2
The blast wave parameters a_n and b_n of Eqs. 9 and 10 for various centralities obtained by fits to the WA98 inclusive photon data (left) and the corresponding parameters extracted for neutral pions (right) from simulations that reproduce the inclusive photon results.

Fig. 5a,b shows k_2, the ratio of the flow coefficients of photons and pions, obtained from the simulations. The k_1 ratio is found to be independent of centrality and p_T with a value of $\langle k_1 \rangle = 1.075 \pm 0.003$ with a systematic error less than $\pm 12\%$. Since v_1^π is small, $k_1 \approx 1$. The k_2 ratios are also found to be independent of centrality with $\langle k_2 \rangle = 1.215 \pm 0.002$ and a systematic error less than $\pm 8\%$, but strongly dependent on p_T. The observation that the k_n ratios are greater than unity can be understood as a simple effect of the π^0 decay and the fact that the v_n increase with p_T. Comparing photons and π^0's at a given p_T, the decay photons will have been produced from π^0's with larger p_T and hence larger v_n, giving $k_n > 1$ (see Fig. 5a and b). The k_n results shown in Fig. 5a and b have been used to estimate the neutral pion flow values from the measured photon flow.

The π^0 v_2 extracted from the measured WA98 photon v_2 as a function of centrality are compared to the results from NA49 for charged pions [42] in Fig. 6. For this comparison the WA98 results for photons with $p_T > 0.18$ GeV/c were corrected to the expectation for the pions without p_T threshold ($p_T > 0$ GeV/c) as for NA49 results with the correction factor $k_1^0 = 1.30 \pm 0.036$ and $k_2^0 = 1.59 \pm 0.003$. The systematic errors on the WA98 points including the errors of the measured photon v_n values and the additional error of the k_n^0 correction are less than $\pm 20\%$, except for the lowest p_T points where the upper systematic errors increase (Fig. 8). The systematic errors on the NA49 data points vary from 13% for the most peripheral to 80% for the most central bin. The two measurements are seen to be in agreement.

The rapidity dependence of the pion flow coefficients is shown in Fig. 7 for two centrality selections. The WA98 photon v_n with $p_T > 0.18$ GeV/c were corrected to the expectation for π^0's without p_T threshold using the correction factors k_n^0 given above. The NA49 results for pions with $p_T > 0$ GeV/c with appropriate corrections ([42]) are also shown and seen to be in agreement. Similar agreement between the two experiments is seen in the transverse momentum dependence of the v_2 shown in Fig. 8.

Fig. 9 shows the WA98 π^0 v_2 coefficient deduced from the measured photon v_2 (corrected by k_2^0) together with a compilation of results [42] from other experiments. Results are shown from E877 [8,12], CERES [44], NA49 [42], PHOBOS [45], PHENIX [46], and STAR [47], The WA98 result follows the general trend of the smooth increase of the elliptic flow with increasing beam energy. It should be kept in mind that the p_T and rapidity coverages as well as centrality selections differ for the various experiments.

Since the strength of the elliptic flow should be proportional to the initial eccentricity of the collision zone, it is useful to normalize the measured v_2 to the eccentricity of the reaction geometry when investigating the systematics of the elliptical flow [48]. The initial spatial eccentricity was calculated within a Glauber model calculation [37] as:

$$\epsilon = \frac{< y^2 > - < x^2 >}{< y^2 > + < x^2 >}$$

where x and y are the participant nucleon coordinates in the plane perpendicular to the beam and x denotes the in-plane direction.

It is of interest to plot the quantity v_2/ϵ versus the particle density as estimated by the dN/dy of charged particles divided by the area of the overlap region S [8,42]. Neglecting the weak incident energy and centrality dependence of the average p_T, the scaled particle density is proportional to the initial energy density in the Bjorken estimate [51]. Fig.10 shows the WA98 result for v_2/ϵ for neutral pions together with results for charged pions from NA49 [42] and results for charged particles from STAR [49,50] and E877 [8]. The RHIC data have been corrected for their p_T cutoff, the errors are statistical. For the WA98 points the dN/dy are taken from WA98 measurements [37].

The WA98 results confirm the previous observation [8,42] of a universal dependence of v_2/ϵ on the particle density. It should be noted that results at different incident energies but similar average particle density correspond to dramatically different collision geometries. Generally, a central collision at low energy will have a particle density similar to a more peripheral collision at higher energy. Thus, the universal dependence demonstrates that the scaled v_2 depends only on the initial energy density, or initial pressure, rather than being

dependent on the particle density times pathlength, which would be the expectation if only partial thermalization was attained. The observed increase of the scaled elliptic flow with increasing particle density is qualitatively similar to that seen in a recent hydrodynamical model study [52] in which the v_2 value for fixed impact parameter increases smoothly with increasing dN_{ch}/dy corresponding to the increase in pressure. That systematic study of hadron spectra and flow results indicated that existing data are best reproduced by hydrodynamic model calculations with an equation of state which include a transition to a Quark Gluon Plasma Phase at a critical temperature of $T_c = 165$ MeV with a latent heat of 800 MeV [52].

7 Summary

Directed and elliptic flow of photons have been measured in 158 A GeV Pb+Pb collisions using the LEDA electromagnetic calorimeter and the Plastic Ball detector of the WA98 experiment. The conventional reaction plane method for directed and elliptic flow and the pair-correlation method for elliptic flow have been used in the analysis. The elliptic flow values obtained by the two methods are consistent.

The centrality and p_T dependences of the photon directed and elliptic flow coefficients were presented. In-plane elliptic flow is observed. Both flow values increase for more peripheral collisions and with increasing p_T.

For comparison with charged pion measurements, the neutral pion flow coefficients have been extracted from the measured photon flow coefficients using Monte Carlo simulations. The Monte Carlo simulations demonstrate that the average photon flow coefficients are $\approx$7–21% greater than the parent π^0 flow coefficients. The extracted neutral pion flow results are compatible with the NA49 charged pion flow and with the general trend of the elliptic flow behaviour as a function of beam energy. The universal dependence of the elliptic flow, scaled by the eccentricity of the initial nuclear overlap, on particle density is confirmed.

References

[1] M. Hofmann et al., Nucl. Phys. **A 566** (1994) 15c.

[2] J.-Y. Ollitrault, Phys. Rev. **D 46** (1992) 229; Phys.Rev. **D 48** (1993), 1132; Nucl.Phys. **A 638** (1998) 195c.

[3] H. Sorge, Phys. Rev. Lett. **78** (1997) 2309.

[4] H. Stocker and W. Greiner, Phys. Rep. **137** (1986) 277.

[5] C.M. Hung and E.V. Shuryak, Phys. Rev. Lett. **75** (1995) 4003.

[6] D.H. Rischke, Nucl. Phys. **A 610** (1996) 88c.

[7] NA49 Collaboration, T. Alber et al., Phys. Rev. Lett. **75** (1995) 3814; WA98 Collaboration, M.M. Aggarwal et al., Eur. Phys. J. **C 18** (2001) 0651; PHENIX Collaboration, K. Adcox et al., Phys. Rev. Lett. **87** (2001) 052301.

[8] S. Voloshin and A. Poskanzer, Phys. Lett. **B 474** (2000) 27.

[9] Plastic Ball Collaboration, H.A. Gustafsson et al., Phys. Rev. Lett. **52** (1984) 1590; H.H. Gutbrod et al., Phys. Lett. **B 216** (1989) 267; Rep. Prog. Phys. **52** (1989) 1267; H.A. Gustafsson et al., Phys. Rev. **C 42** (1990) 640.

[10] KAOS Collaboration, D. Brill et al., Phys. Rev. Lett. **71** (1993) 336; Z. Phys. **A 355** (1996) 61; Z. Phys. **A 357** (1996) 207; Y. Shin, Phys. Rev. Lett. **81** (1998) 1576.

[11] FOPI Collaboration, G. Poggi et al., Nucl. Phys. **A 586** (1995) 755; J.L. Ritman et al., Z. Phys. **A 352** (1995) 355; N. Bastid et al., Nucl. Phys. **A 622** (1997) 573.

[12] E877 Collaboration, J. Barette et al., Phys. Rev. Lett. **70** (1993) 2996; Phys. Rev. Lett. **73** (1994) 2532; Phys. Rev. **C 55** (1997) 1420; Phys. Rev. **C 56** (1997) 3254; S.A. Voloshin et al., Nucl.Phys. **A 638** (1998) 455c.

[13] NA49 Collaboration, T. Wienold et al., Nucl. Phys. **A 610** (1996) 76c; H. Appelshauser et al., Phys. Rev. Lett. **80** (1998) 4136; A.M. Poskanzer et al., Nucl. Phys. **A 638** (1998) 463c; A.M. Poskanzer et al., Nucl. Phys. **A 661** (1999) 341c; A. Wetzler et al., Nucl. Phys. **A 715** (2003) 583c.

[14] WA80 Collaboration, T.C. Awes et al., Phys. Lett. **B 381** (1996) 29.

[15] WA93 Collaboration, M.M. Aggarwal et al., Phys. Lett. **B 403** (1997) 390.

[16] WA98 Collaboration, M. Kurata et al., Prog. Theor. Phys. Suppl. **129** (1997) 179; B. Wyslouch et al., Nucl. Phys. **A 638** (1998) 147c; S. Nishimura et al., Nucl. Phys. **A 638** (1998) 459c; S. Nishimura et al., Nucl. Phys. **A 661** (1999) 464c; M.M. Aggarwal et al., nucl-ex/9807004; M.M. Aggarwal et al., Phys. Lett. B 469 (1999) 30; S. Nishimura et al., Nucl. Phys. **A 663-664** (2000) 729c;

[17] CERES Collaboration, G. Agakichiev et al., Phys. Rev. Lett. **92** (2004) 032301;

[18] PHENIX Collaboration, K. Adcox et al., Phys. Rev. Lett. **89** (2002) 212301; S. Esumi et al., nucl-ex/0210012.

[19] STAR Collaboration, K.H. Ackermann et al., Phys. Rev. Lett. **86** (2001) 402; C. Adler et al., Phys. Rev. Lett. **87** (2001) 182301.

[20] PHOBOS Collaboration, B. Back et al., nucl-ex/0406021.

[21] WA98 Collaboration, S. Nikolaev et al., Nucl. Phys. **A 715** (2003) 579c.

[22] WA98 Collab., S. Bathe et al., Nucl. Phys. **A 715** (2003) 729c.

[23] WA98 Collaboration, *Proposal for a large acceptance hadron and photon spectrometer*, 1991, Preprint CERN/SPSLC 91-17, SPSLC/P260.

[24] T.C. Awes et.al., Nucl. Instr. Meth. Phys. Res. Sect. **A 279** (1989) 479.

[25] A. Baden et.al., Nucl. Instr. Meth. Phys. Res. Sect. **A 203** (1982) 189.

[26] WA98 Collaboration, M.M. Aggarwal et al., nucl-ex/0006007 (2000).

[27] S. Neumaier et al., Nucl. Instr. Meth. Phys. Res. Sect. **A 360**, 593 (1995).

[28] A.L. Wintenberg et al., Proceedings of Electronics for Future Colliders Conference, May 1994, LeCroy Corp.

[29] T. Peitzmann et al., Nucl. Instr. Meth. Phys. Res. Sect. **A 376**, 368 (1996).

[30] S. Voloshin and Y. Zhang, Z. Phys. **C 70** (1996) 665.

[31] A. Poskanzer and S. Voloshin, Phys. Rev. **C 58** (1998) 1671.

[32] WA98 Collaboration, H. Schlagheck et al., Nucl. Phys. **A 661** (1999) 337c.

[33] S. Wang et al., Phys. Rev. **C 44** (1991) 1091.

[34] R. Lacey et al., Phys. Rev. Lett. **70** (1993) 1224.

[35] R. Lacey PHENIX Collaboration Nucl.Phys. **A 698** (2002) 559.

[36] N. Borghini et al., Phys. Rev. **C 64** (2001) 054901.

[37] WA98 Collaboration, M.M. Aggarwal et al., Eur. Phys. J. **C 18** (2001) 651–663.

[38] WA98 Collaboration, M.M. Aggarwal et al., Eur. Phys. J. **C 23** (2002) 225–236.

[39] F. Berger et al., Nucl. Instr. Meth. Phys. Res. Sect. **A 321** (1992) 152.

[40] P. Danielewicz and G.Odyniec, Phys. Lett. **B 157** (1985) 146.

[41] H. Büsching, PhD Thesis, Universitat Münster, 2002.

[42] NA49 Collab., C .Alt et al., Phys. Rev. **C 68** (2003) 034903.

[43] P .Huovinen et al., Phys. Lett. **B 503** (2001) 58.

[44] CERES Collab., K. Filimonov et al., nucl-ex/0109017.

[45] PHOBOS Collaboration, S. Manly et al., Nucl. Phys. **A 715** (2003) 611c.

[46] PHENIX Collaboration, S. Esumi et al., Nucl. Phys. **A 715** (2003) 599c.

[47] STAR Collaboration, L. Ray et al., Nucl. Phys. **A 715** (2003) 45c.

[48] H. Sorge, Phys. Rev. Lett. **82** (1999) 2048.

[49] STAR Collaboration, L. Ray,Quark Matter'02, Nucl. Phys. **A 715** (2003) 45c.

[50] STAR Collaboration, C. Adler et al., Phys. Rev. **C 66** (2002) 034904.

[51] J.D. Bjorken, Phys. Rev. **D 27** (1983) 140.

[52] D. Teaney, J. Lauret, and E.V. Shuryak et al., nucl-th/0110037.

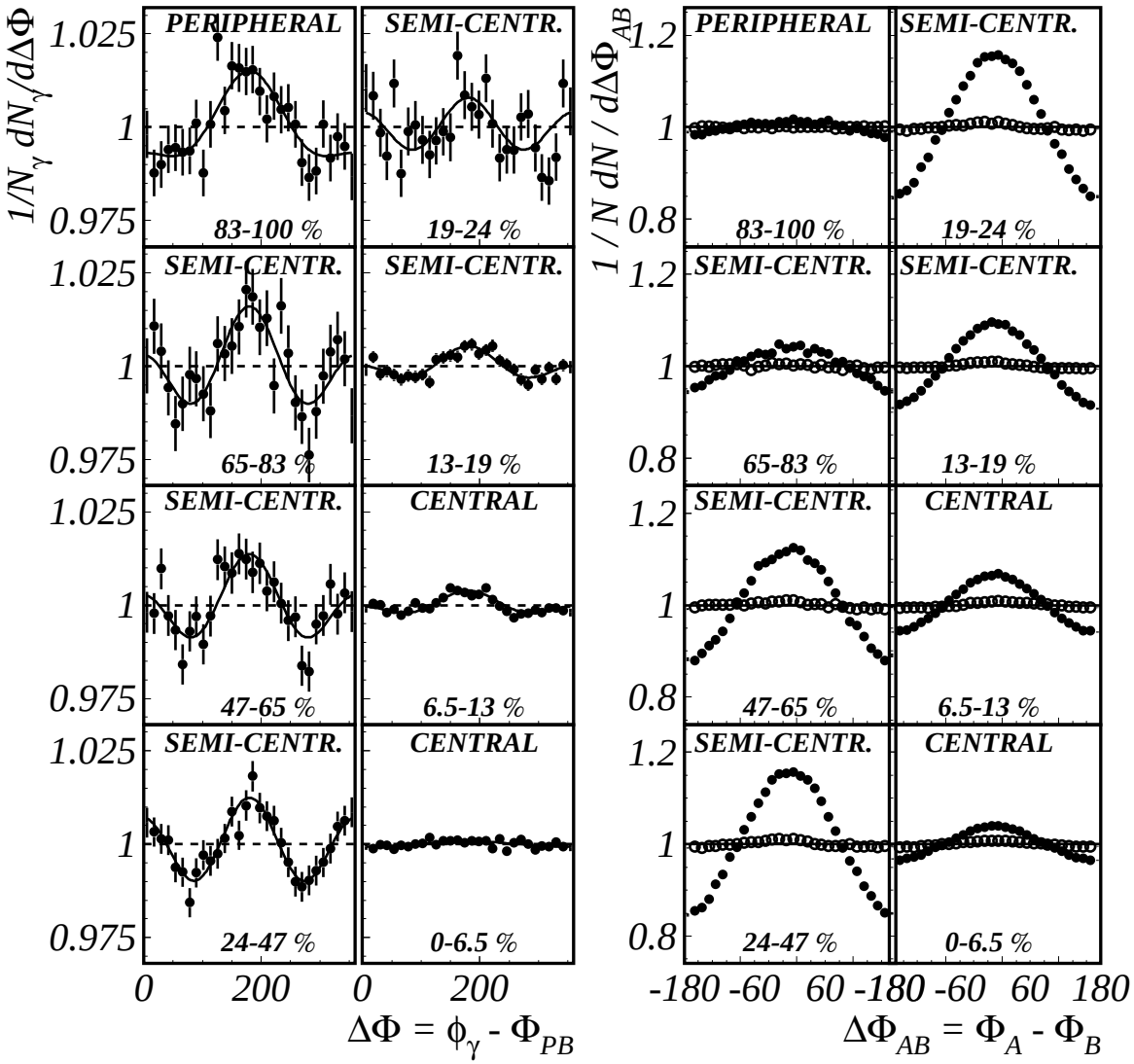

Fig. 1. Left: The measured photon azimuthal correlation functions for different centralities. The solid lines show fits to equation 3. Right: Subevent correlation functions of particles measured in the Plastic Ball for different centralities. The filled circles show the measured correlation functions. The open circles show the results for mixed subevents.

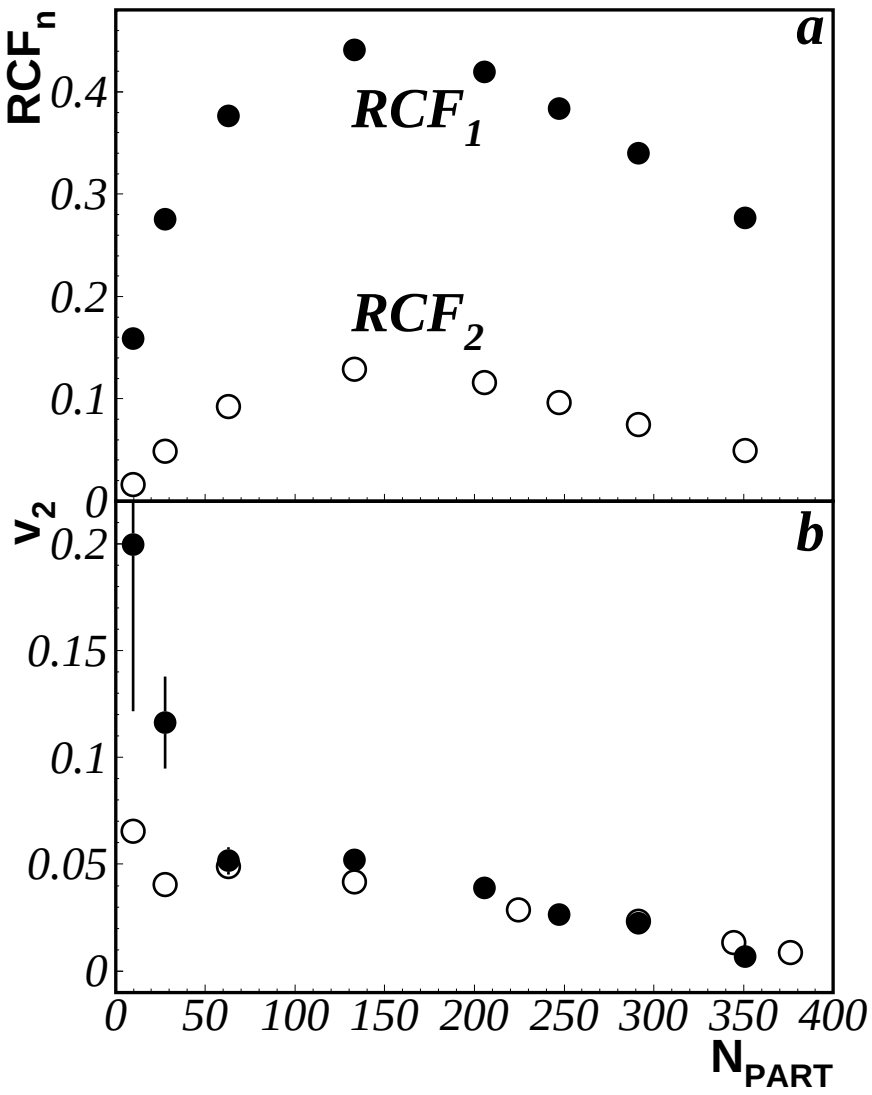

Fig. 2. (a) The resolution correction factors obtained from subevent correlation functions of particles measured in the target fragmentation region as a function of the number of participants. The filled circles show the values for directed flow, the open circles for elliptic flow. (b) The elliptic flow v_2 of photons extracted by the reaction plane method (solid circles, $p_T \geq 0.18$ GeV/c) and by the correlation method (open circles, $p_{T1} \geq 0.18$ GeV/c, $p_{T2} \geq 0.18$ GeV/c), integrated over $p_T > 0.18$ GeV/c and y =2.3–2.9 as a function of the number of participants.

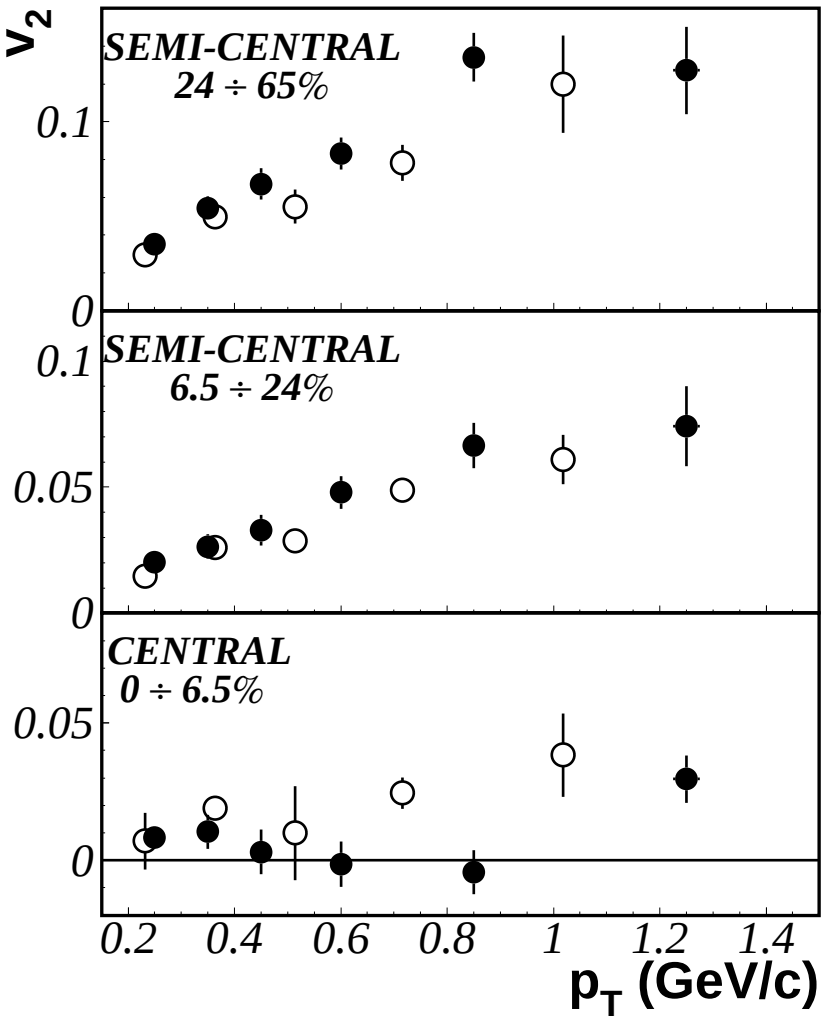

Fig. 3. The elliptic flow v_2 of photons extracted by the reaction plane method (solid circles, $p_T \geq 0.18$ GeV/c) and by the correlation method (open circles, $p_{T1} \geq 0.18$ GeV/c, $p_{T2} \geq 0.18$ GeV/c), integrated over y =2.3–2.9 for three centrality selections.

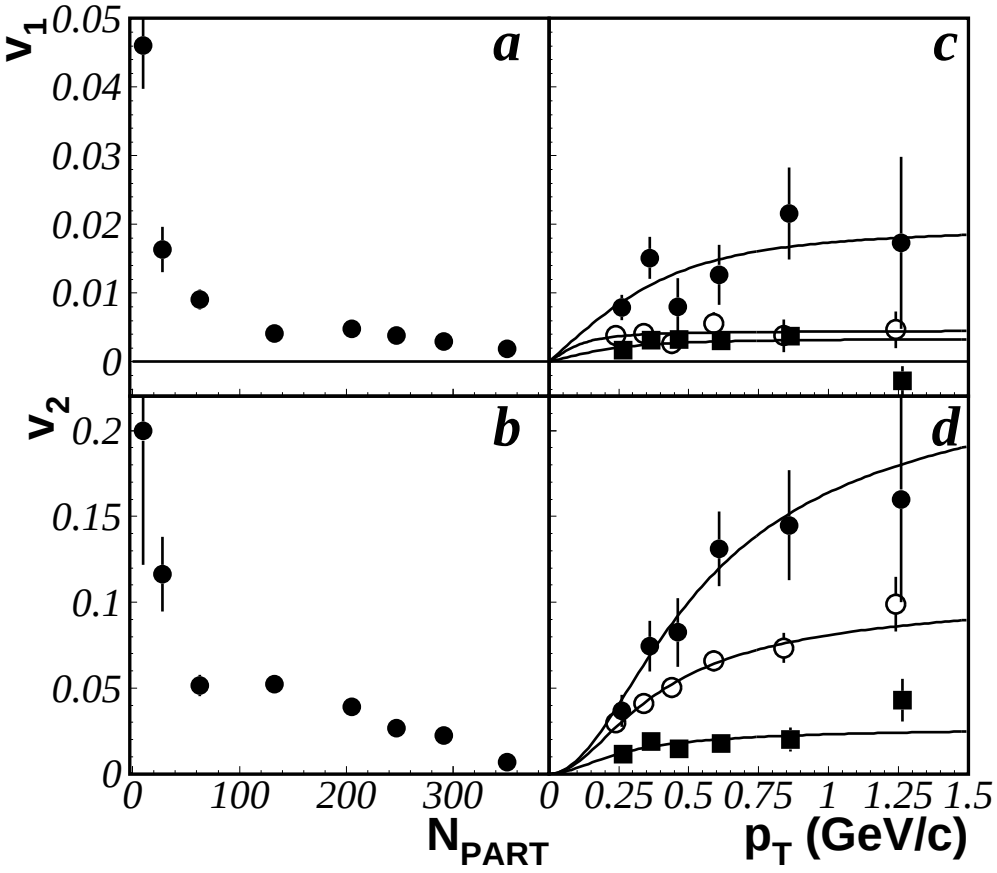

Fig. 4. Directed flow (v_1) (a) and elliptic flow (v_2) (b) of photons integrated over $p_T > 0.18$ GeV/c and $y = 2.3 - 2.9$ as a function of the number of participants. Directed flow (v_1) (c) and elliptic flow (v_2) (d) of photons integrated over y =2.3–2.9 as a function of p_T for various centralities. Solid circles show results for semi-central events (47–83%), open circles show results for semi-central events (13–47%), solid squares show results for central events (0–13%). Solid lines are fitted results to a blast wave model functional form.

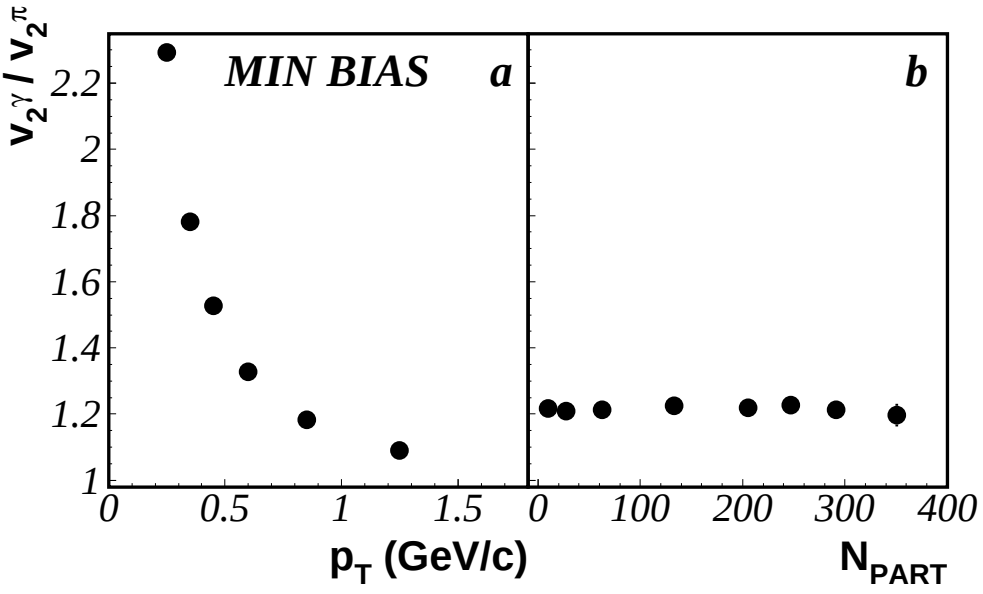

Fig. 5. The ratio of photon elliptic flow to parent pion elliptic flow coefficients. (a) $k_2 = v_2^\gamma / v_2^\pi$ for min. bias, (b) $k_2 = v_2^\gamma / v_2^\pi$ for different centrality bins.

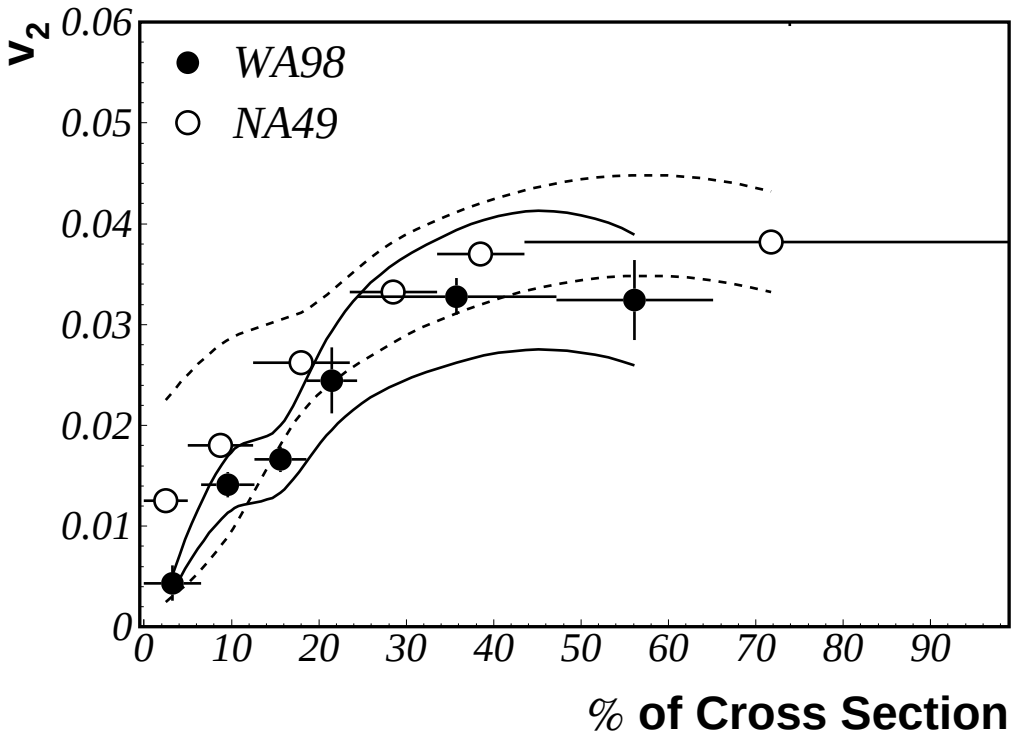

Fig. 6. The centrality dependence of pion elliptic flow v_2 extracted from the measured photon flow from WA98 (solid circles, $-0.6 < y_{CM} < 0$), compared to pion flow results of NA49 (open circles, $0 < y_{CM} < 2.1$, [42]).

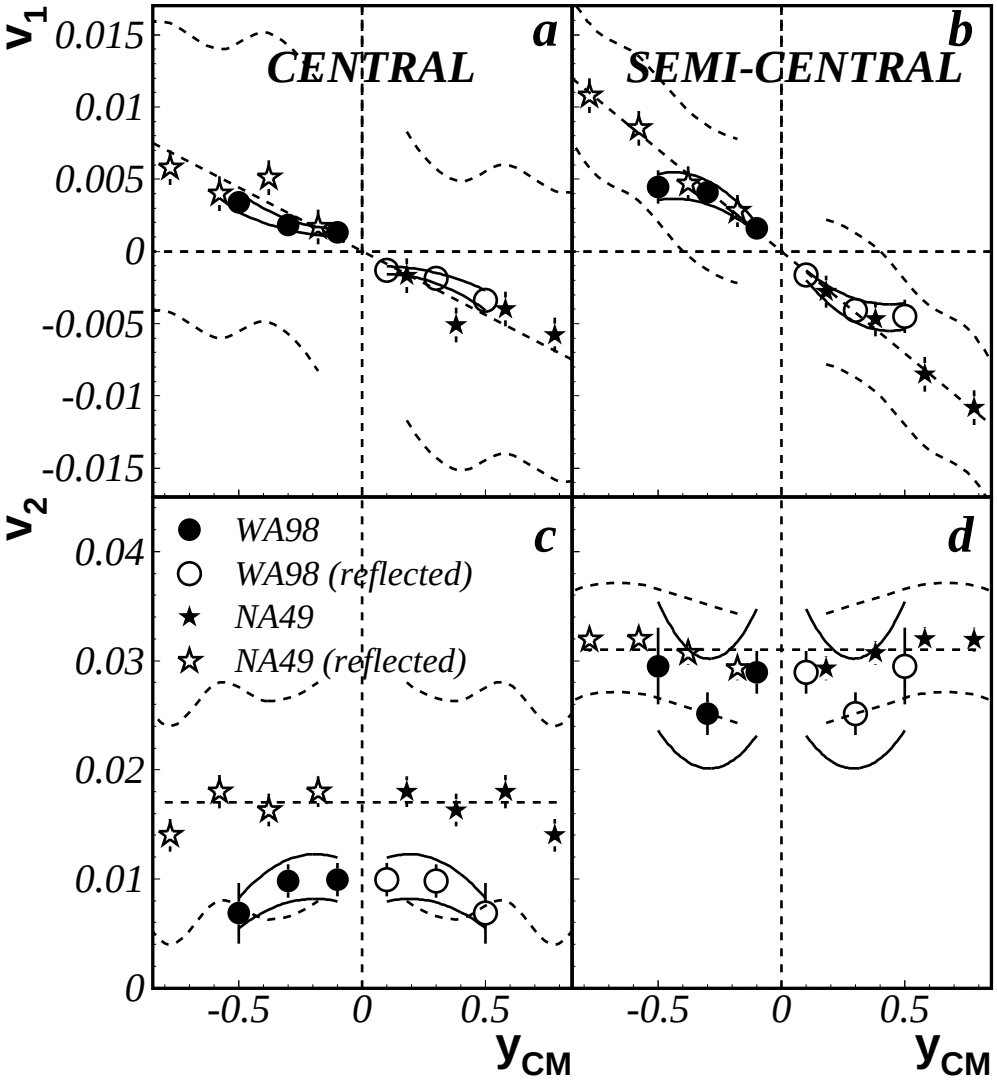

Fig. 7. The rapidity dependence of pion flow extracted from the measured photon flow from WA98 (circles) compared to pion flow results of NA49 (stars, [42]). The results are shown for central on the left panel (WA98: 0–13%, NA49: 0–12.5%) and semi-central on the right panel (WA98: 13–47%, NA49: 12.5–33.5%) selections for the directed flow (a,b) and elliptic flow (c,d). Systematic error bands are shown on (c) for NA49 (dashed curves) and for WA98 (solid curves). Open points are reflected at mid-rapidity. The dashed lines indicating the rapidity dependence are only meant to guide the eye.

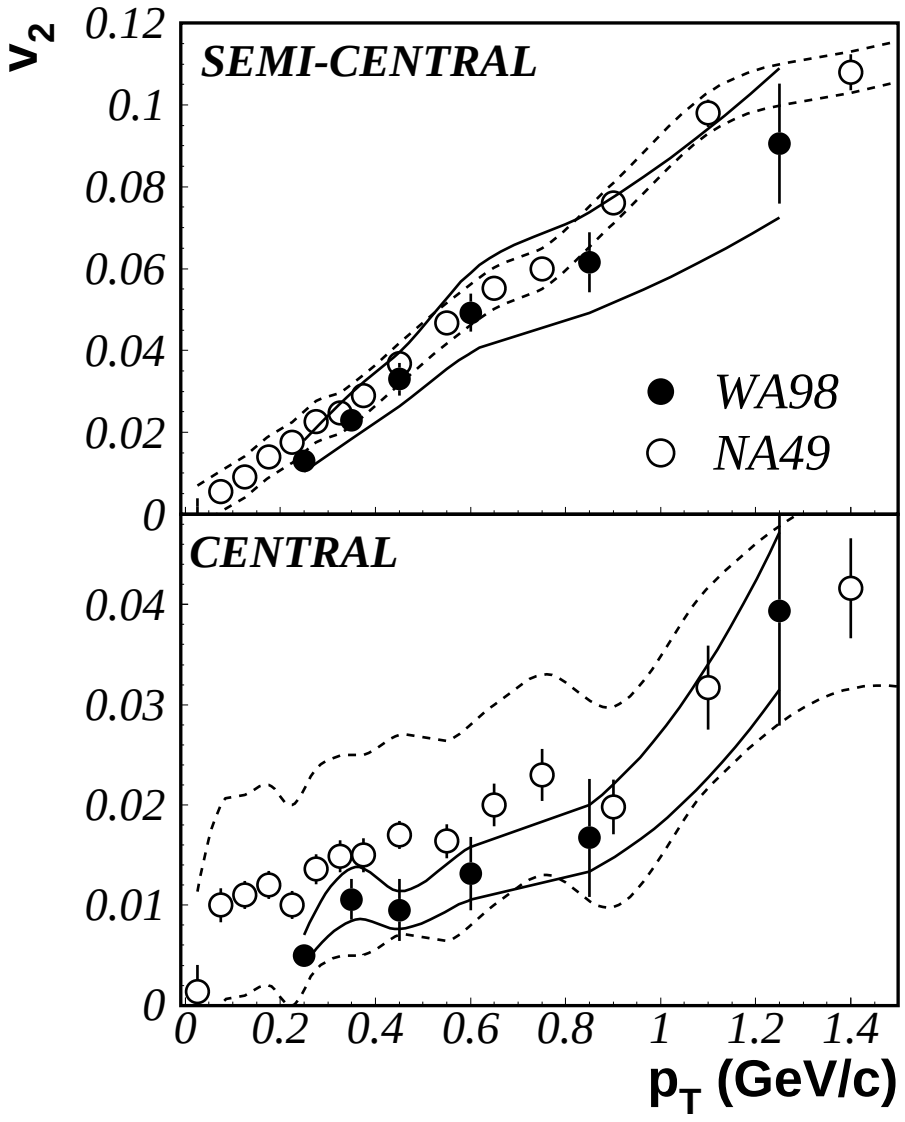

Fig. 8. The transverse momentum dependence of the π^0 elliptic flow extracted from the measured photon flow from WA98 (solid circles) compared to π^+ elliptic flow results of NA49 (open circles, [42]). The results are shown for semi-central selections (top: WA98: 13–47%, $-0.6 < y_{CM} < 0$, NA49: 12.5–33.5%, $0 < y_{CM} < 0.8$) and for central selections (Bottom: WA98: 0–13%, $-0.6 < y_{CM} < 0$, NA49: 0–12.5%, $0 < y_{CM} < 0.8$). Systematic error bands are shown for NA49 (dashed curves) and for WA98 (solid curves).

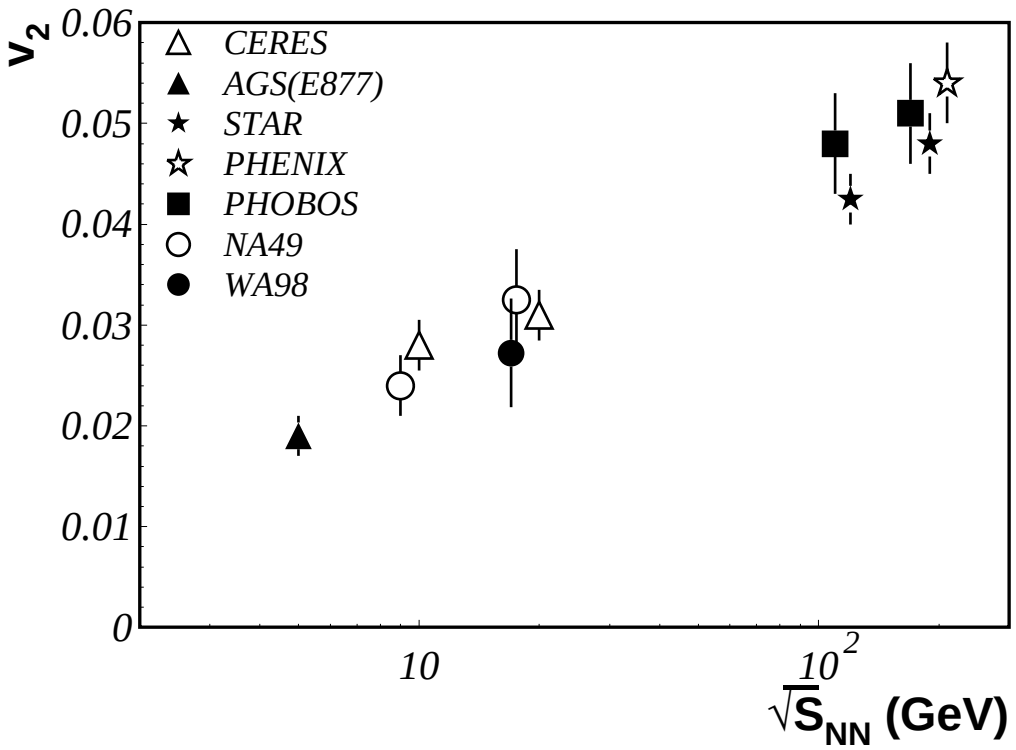

Fig. 9. Comparison of the WA98 p_T-integrated elliptic flow results at $\sqrt{s_{NN}} = 17$ GeV (13–47%, $-0.6 < y_{CM} < 0$) with results from other experiments for different collision energies. The WA98 result is the π^0 elliptic flow extracted from the measured photon elliptic flow, as described in the text. The total statistical and systematic error is shown on the WA98 point.

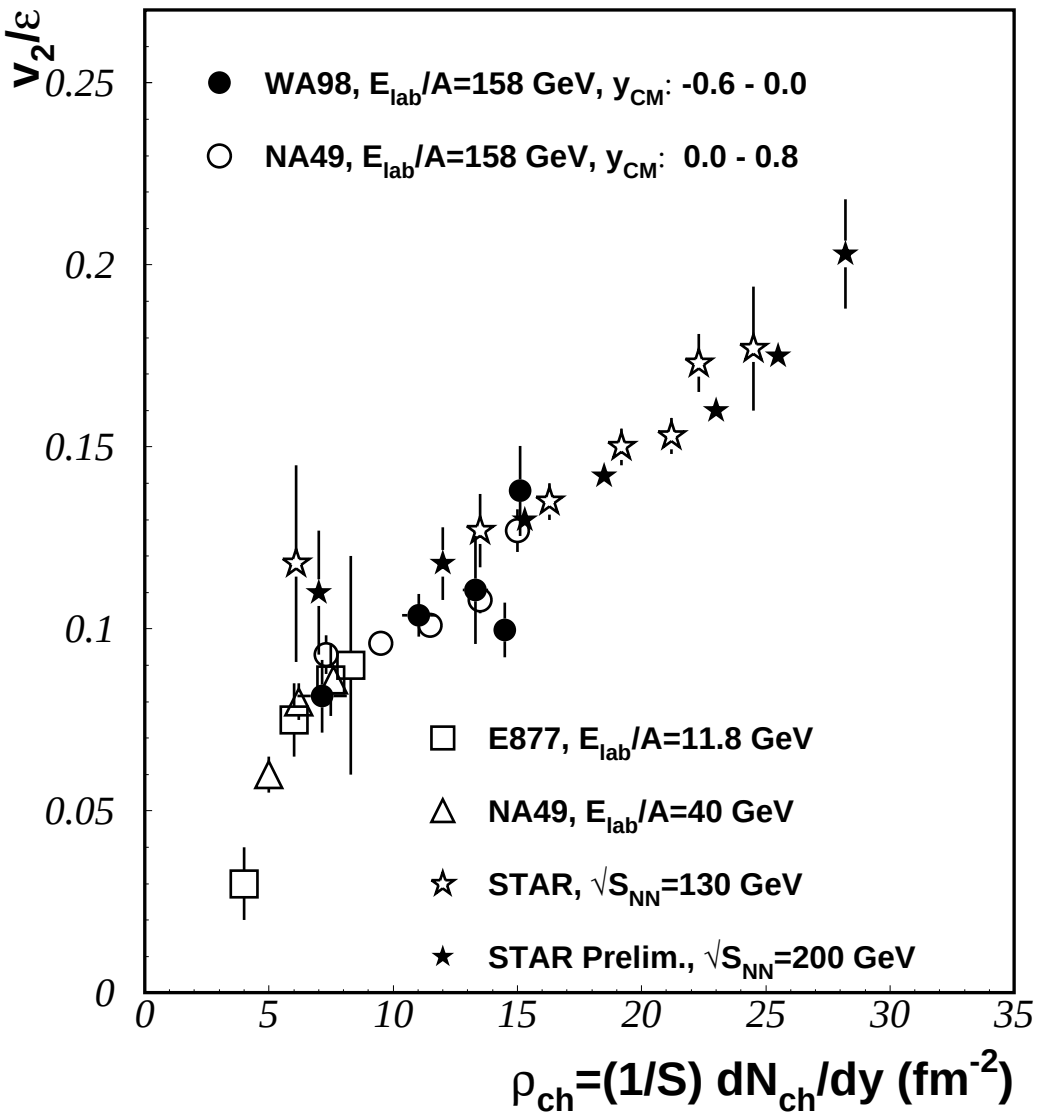

Fig. 10. The scaled elliptic flow v_2/ϵ as a function of particle density. Results are shown for the WA98 p_T-integrated v_2 values at $\sqrt{s_{NN}} = 17$ GeV ($-0.6 < y_{CM} < 0$). The WA98 results are compared to results from the E877, NA49, and STAR experiments. The WA98 result is the π^0 elliptic flow extracted from the measured photon elliptic flow, as described in the text.